

## Hydrogen trapping in oxygen-deficient hafnium silicates

L. R. C. Fonseca, A. L. Xavier Jr., M. Ribeiro Jr., C. Driemeier, and I. J. R. Baumvol

Citation: *Journal of Applied Physics* **102**, 044108 (2007); doi: 10.1063/1.2769790

View online: <http://dx.doi.org/10.1063/1.2769790>

View Table of Contents: <http://scitation.aip.org/content/aip/journal/jap/102/4?ver=pdfcov>

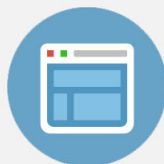
Published by the [AIP Publishing](#)

---



## Re-register for Table of Content Alerts

Create a profile.



Sign up today!



## Hydrogen trapping in oxygen-deficient hafnium silicates

L. R. C. Fonseca,<sup>a)</sup> A. L. Xavier, Jr., and M. Ribeiro, Jr.

*Wernher von Braun Center for Advanced Research, Av. Perimetral Norte 301, Campinas, SP 13098-381, Brazil*

C. Driemeier

*Instituto de Física, Universidade Federal do Rio Grande do Sul, Porto Alegre, RS 91501-970, Brazil*

I. J. R. Baumvol

*CCET, Universidade de Caxias do Sul, Caxias do Sul, RS 95070-560, Brazil and Instituto de Física, Universidade Federal do Rio Grande do Sul, Porto Alegre, RS 91501-970, Brazil*

(Received 30 May 2007; accepted 30 June 2007; published online 23 August 2007)

Isotopic substitution, nuclear reaction analysis, and x-ray photoelectron spectroscopy were employed to show that oxygen-deficient hafnium (Hf) silicates trap hydrogen atoms. Based on this experimental observation, we used first-principles calculations to investigate the structure, energetics, and electronic properties of H interacting with O vacancies in a hafnium silicate model. We found that O vacancies close to a Si atom are energetically favored when compared to vacancies in HfO<sub>2</sub>-like regions, implying that close-to-Si O vacancies are more likely to occur. Trapping of two H atoms at a close-to-Si O vacancy passivates the vacancy-induced gap states. The first H interacts with neighboring Hf atoms, whereas the second H binds to the Si atom. © 2007 American Institute of Physics. [DOI: 10.1063/1.2769790]

### I. INTRODUCTION

Continuous scaling of metal–oxide–semiconductor field-effect transistors (MOSFETs) led traditional SiO<sub>2</sub> and SiO<sub>x</sub>N<sub>y</sub> gate dielectric films to approach 1 nm thickness in Si-based integrated circuit technologies. Further MOSFET scaling is severely limited by an exponential increase in leakage currents through the gate dielectric due to direct electron tunneling. In order to overcome this limitation, high dielectric constant (high-*k*) materials will replace SiO<sub>2</sub> and SiO<sub>x</sub>N<sub>y</sub>.<sup>1–3</sup> High-*k* materials allow physically thicker films, which reduce leakage currents, while still increasing MOSFET capacitance density, as required for further MOSFET scaling. Hafnium silicates, which are (SiO<sub>2</sub>)<sub>x</sub>(HfO<sub>2</sub>)<sub>1–x</sub> mixed oxides (HfSiO, for short), are attractive high-*k* candidates due to possible compositional tuning between high-quality SiO<sub>2</sub> and high-*k* HfO<sub>2</sub>.<sup>4,5</sup>

For SiO<sub>2</sub> gate dielectrics, the presence of H is necessary for the passivation of electrically active Si dangling bonds at the SiO<sub>2</sub>/Si interface.<sup>6</sup> On the other hand, H has detrimental roles in negative-bias-temperature instabilities,<sup>7</sup> radiation-induced instabilities,<sup>8</sup> stress-induced leakage current,<sup>9,10</sup> and hot-electron degradation.<sup>11</sup> For HfO<sub>2</sub> gate dielectrics, similar H passivation of interface Si dangling bonds was observed<sup>12,13</sup> and interstitial H (Refs. 14 and 15) as well as H-passivated O vacancy<sup>16</sup> were proposed as positive charge centers. Further, previous studies showed that typical H concentrations in Hf-based oxide films deposited on Si(10<sup>21</sup>–10<sup>22</sup> cm<sup>-3</sup>) (Refs. 17–19) are much higher than in bulk-like regions of SiO<sub>2</sub> thermally grown on Si(10<sup>18</sup>–10<sup>19</sup> cm<sup>-3</sup>).<sup>20–22</sup> This scenario suggests that H plays significant roles in HfSiO gate dielectrics.

In this work, H trapping in oxygen-deficient HfSiO is investigated. First, sequential annealing of HfSiO films in vacuum, oxygen, and deuterium (<sup>2</sup>H<sub>2</sub>) was performed. Then, nuclear reaction analysis and x-ray photoelectron spectroscopy were employed to show that <sup>2</sup>H incorporation is related to O deficiency in the HfSiO films. Finally, first-principles calculations were performed in a HfSiO model structure with H interacting with O vacancies. The structure, energetics, and electronic properties of vacancy-hydrogen complexes are presented. Links between experiment and theory are discussed.

### II. EXPERIMENTAL RESULTS

HfSiO films 4, 6, 8, and 10 nm thick with 30% SiO<sub>2</sub> concentration, i.e., (SiO<sub>2</sub>)<sub>0.3</sub>(HfO<sub>2</sub>)<sub>0.7</sub> composition, were deposited on Si(100) by metalorganic chemical vapor deposition at 650 °C using Hf[N(C<sub>2</sub>H<sub>5</sub>)<sub>2</sub>]<sub>4</sub> and Si[N(CH<sub>3</sub>)<sub>2</sub>]<sub>4</sub> precursors and O<sub>2</sub> as the oxygen source. Postdeposition annealing was performed in a Joule-effect heated furnace whose quartz tube was pumped down to a base pressure of 10<sup>-7</sup> mbar. Each annealing was run for 30 min, either in vacuum or in a static gaseous atmosphere, viz., 1 mbar O<sub>2</sub> or 60 mbar <sup>2</sup>H<sub>2</sub> (H<sub>2</sub> 95% enriched in the <sup>2</sup>H isotope). Vacuum and O<sub>2</sub> annealing were performed at 800 °C, whereas <sup>2</sup>H<sub>2</sub> annealing was performed at 500 °C. Using <sup>2</sup>H<sub>2</sub> is convenient because it chemically mimics H<sub>2</sub> with natural isotopic abundances (99.985% <sup>1</sup>H) and allows distinguishing H atoms incorporated from the annealing atmosphere (<sup>2</sup>H) from those previously existing in the films or incorporated from air (<sup>1</sup>H).

<sup>2</sup>H areal densities in the HfSiO films were determined using 400 keV <sup>3</sup>He<sup>+</sup> beams to induce the <sup>2</sup>H(<sup>3</sup>He, *p*)<sup>4</sup>He nuclear reaction.<sup>23</sup> This nuclear reaction technique relies on (i) the low H solubility in *c*-Si,<sup>24</sup> which leads to negligible

<sup>a)</sup>Author to whom correspondence should be addressed. Electronic mail: [fonseca@vonbraunlabs.com.br](mailto:fonseca@vonbraunlabs.com.br)

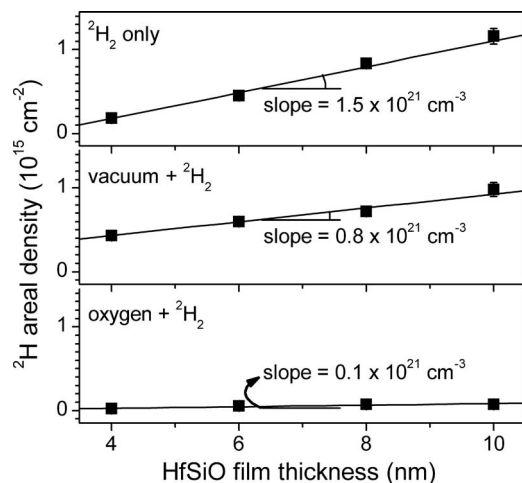


FIG. 1.  $^2\text{H}$  areal densities versus HfSiO film thickness after annealing in  $^2\text{H}_2$ , either without (top) or with preannealing in vacuum (middle) or oxygen (bottom). The slopes were derived by linear fitting (solid lines), corresponding to bulk-like  $^2\text{H}$  concentrations.

contribution ( $<10^{12} \text{ cm}^{-2}$ ) from  $^2\text{H}$  in the Si substrate, and (ii) nuclear reaction cross section constant throughout the films,<sup>25</sup> which implies nuclear reaction yield proportional to  $^2\text{H}$  areal density. By comparison with a  $^2\text{H}$ -implanted sample with known  $^2\text{H}$  areal density, the  $^2\text{H}$  areal densities in the HfSiO films are determined.

Figure 1 shows  $^2\text{H}$  areal densities as a function of HfSiO film thickness after annealing in  $^2\text{H}_2$ , either with or without preannealing. One observes  $^2\text{H}$  areal densities increasing with film thickness, indicating  $^2\text{H}$  incorporation in bulk regions of the HfSiO films. This is in contrast to H incorporation in HfO<sub>2</sub>/Si thin film structures, where H incorporates mainly close to the HfO<sub>2</sub> surface,<sup>18,26</sup> and in contrast to SiO<sub>2</sub>/Si structures, where H incorporates mainly in the SiO<sub>2</sub>/Si interface region.<sup>22,23</sup> The slopes derived from fitting the data with straight lines are also shown in Fig. 1, expressing bulk-like  $^2\text{H}$  concentrations (in units of atoms per cubic centimeters). One observes a marked decrease in bulk-like  $^2\text{H}$  concentration when preannealing was performed before  $^2\text{H}_2$  exposure. The decrease is more pronounced for the case of preannealing performed in O<sub>2</sub>.

The impact of preannealing on film chemistry was investigated by x-ray photoelectron spectroscopy using a Mg *K* $\alpha$  x-ray source and photoelectron detection at 30° takeoff angle (relative to sample normal). Figure 2 shows photoelectron spectra for the as-deposited and annealed 10 nm HfSiO films. The Hf 4*f* signal (inset) does not present a detectable ( $>0.1 \text{ eV}$ ) shift<sup>27</sup> after annealing in O<sub>2</sub>, indicating no detectable change in the Hf oxidation state. On the other hand, the Si 2*p* signal shifts 0.3 eV (Ref. 27) toward higher binding energies after O<sub>2</sub> annealing. Substrate Si oxidation cannot be responsible for this Si 2*p* shift because the 10 nm films are thick enough to attenuate photoelectrons coming from the HfSiO/Si interface, as evidenced by the absence of substrate Si 2*p* signal at 99.6 eV. This Si 2*p* shift indicates the presence of suboxidized Si atoms converted into higher oxidation states (probably full Si oxidation) by the O<sub>2</sub> annealing. That is to say that the as-deposited and vacuum-annealed HfSiO films are O deficient, which correlates with the pronounced

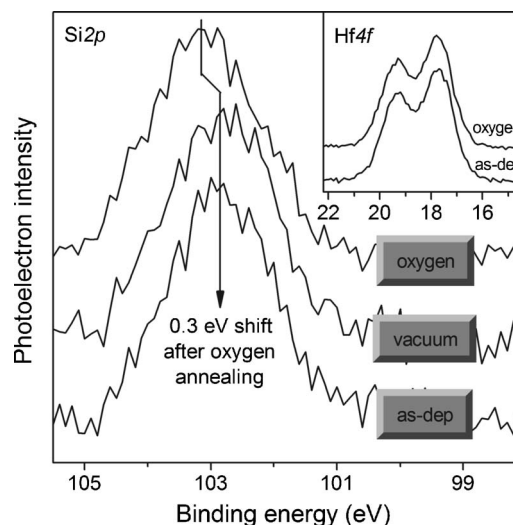


FIG. 2. Photoelectron spectra in the Si 2*p* and Hf 4*f* (inset) regions taken from as-deposited and 800 °C annealed films.

$^2\text{H}$  incorporation observed in these films (see Fig. 1). Annealing in O<sub>2</sub> presumably eliminates the O-deficient sites responsible for  $^2\text{H}$  trapping, leading to the observed decrease in  $^2\text{H}$  incorporation when O<sub>2</sub> preannealing was performed.

### III. THEORETICAL DETAILS

The structure, energetics, and electrical properties of H in HfSiO and HfO<sub>2</sub> were investigated using the generalized gradient approximation<sup>28</sup> of density functional theory (DFT),<sup>29</sup> with core electrons replaced by pseudopotentials (PP), and valence states described by a basis set comprised of linear combinations of numerical atomic orbitals (LCAO) as implemented in the SIESTA code.<sup>30</sup> The double zeta plus polarization basis set was used for the LCAO. Norm-conserving, nonlocal PPs<sup>31</sup> of the Troullier and Martins type<sup>32</sup> were used for all the atomic species. Relativistic PPs for Hf were generated for the neutral atomic configuration  $6s^2 5d^2$ . The alternative configuration  $6s^1 5d^3$  was also employed, with negligible impact on the calculated results. Sampling of *k*-space was done using a  $4 \times 4 \times 4$  *k* point Monkhorst-Pack grid based on the  $(2 \times 2 \times 2)$  *m*-HfO<sub>2</sub> and HfSiO unit cell vectors. All structures considered here have zero net charge.

The calculated cell vectors of the *m*-HfO<sub>2</sub> phase using the primitive 12 atom unit cell ( $a=5.153 \text{ \AA}$ ,  $b=5.198 \text{ \AA}$ ,  $c=5.295 \text{ \AA}$ , and  $\beta=99.74^\circ$ ) are within typical local density approximation/DFT error<sup>33</sup> from experimental data [ $a=5.117 \text{ \AA}$ ,  $b=5.175 \text{ \AA}$ ,  $c=5.295 \text{ \AA}$ , and  $\beta=99.18^\circ$  (Ref. 34)]. For HfSiO we used a 96 atom unit cell (twice the original *m*-HfO<sub>2</sub> primitive unit cell in each direction) with Si atoms replacing Hf atoms. By using a conjugate gradient algorithm, ionic forces were minimized until they were below 0.05 eV/Å. When investigating H and H<sub>2</sub> interstitials, which might be trapped at a local minimum, molecular dynamics (initial heating to 1000 K followed by a slow thermal quenching) was employed to check the final configuration of the system. In all cases tested, the conjugate gradient and molecular dynamics results coincided. The energies of

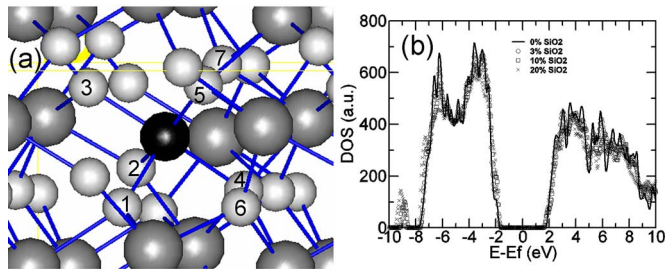


FIG. 3. (Color online) (a) HfSiO model structure showing O (light gray), Hf (dark gray), and Si (black) atoms. (b) Density of states for HfSiO with different SiO<sub>2</sub> concentrations. Fermi level at 0 eV.

chemical reactions were determined by subtracting total energies calculated for reactants from total energies calculated for products.

## IV. THEORETICAL RESULTS

### A. Bulk properties

In the *m*-HfO<sub>2</sub> structure, each Hf atom forms seven Hf–O bonds (2.11–2.23 Å),<sup>35</sup> from which four/three bonds are with threefold/fourfold coordinated O atoms. In the Hf–SiO model with one Si atom replacing one Hf atom, the Si atom is bonded to five O atoms. O6 and O7 [see Fig. 3(a)], which were fourfold coordinated in HfO<sub>2</sub>, become threefold coordinated in HfSiO because they lack a bond to Si (O6 and O7 are 2.06 and 2.91 Å apart from Si). The five Si–O bonds in this HfSiO model (1.80–1.98 Å) are longer than Si–O bonds in amorphous SiO<sub>2</sub>,<sup>36,37</sup> amorphous HfSiO,<sup>38</sup> and crystalline HfSiO<sub>4</sub> (Ref. 39) (~1.60 Å). This difference in bond lengths indicates Si–O bonds affected by the HfO<sub>2</sub> structure where the Si atom was inserted. Although this is a limitation of the model in describing amorphous or SiO<sub>2</sub>-rich hafnium silicates, where Si–O bonds might resemble Si–O bonds in SiO<sub>2</sub>, the model is realistic in describing HfO<sub>2</sub>-rich hafnium silicates, where Si–O bonding is indeed constrained by a HfO<sub>2</sub>-like environment.

Table I shows the calculated lattice parameters and the average coordination numbers for zero, one, three, six, nine, and twelve substitutional Si atoms per unit cell, approximately corresponding, respectively, to 0%, 3%, 10%, 20%, 30%, and 40% SiO<sub>2</sub> concentrations. The numbers in Table I can only offer a general trend as they depend somewhat on the location of the Hf atoms chosen to be replaced by Si. For increasing SiO<sub>2</sub> concentration one observes a trend toward

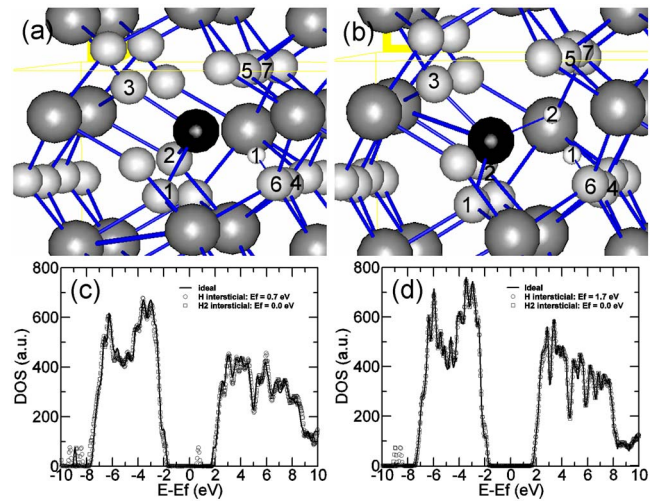


FIG. 4. (Color online) Model structures of (a) HfSiO with interstitial H and (b) HfSiO with interstitial H<sub>2</sub>, with H atoms shown in white. Density of states of (c) HfSiO and (d) HfO<sub>2</sub> with interstitial H and H<sub>2</sub>. Energy scale ( $E-E_f$ ) defined relative to the Fermi level ( $E_f$ ) of the ideal structures.

lower average coordination, which is related to increasing resilience to crystallization.<sup>40</sup> However, the Si coordination seems to saturate at about five, indicating that, as discussed earlier, the present model does not adequately describe SiO<sub>2</sub>-like environments, where Si coordination is four.

Figure 3(b) shows the densities of states (DOS) of HfSiO with different SiO<sub>2</sub> concentrations. In all cases the band gap is clean. Its value of ~3.7 eV is lower than the experimental gap of ~5.7 eV (Ref. 41) due to an intrinsic limitation of DFT to properly deal with excited states. The appearance of a peak at -9 eV and the small peaks at the conduction band minimum (CBM) are associated with Si atoms. Hereafter only the HfSiO model with ~3% SiO<sub>2</sub> concentration (one Si atom) is considered.

### B. Interstitial H and H<sub>2</sub>

We first consider the case of H and H<sub>2</sub> interstitials in HfSiO. An interstitial H atom at a close-to-Si site bonds to O6 [O6–H=1.04 Å, Si–H distance is 1.90 Å, see Fig. 4(a)], recovering O6 original coordination of four. The energy of the O6–H configuration is 5 meV lower than the O7–H. The presence of H increases Si separation from O4 and O5 to 2.35–2.52 Å, breaking these bonds (which were the longest Si–O bonds) and reducing the coordination of O4

TABLE I. Structural parameters for different SiO<sub>2</sub> concentrations in HfSiO. The length of the HfO<sub>2</sub> (0% SiO<sub>2</sub>) unit cell vectors was doubled to facilitate comparison.

SiO <sub>2</sub> concentration (%)	Lattice length (Å)			Lattice angles (deg)			Average atomic coordination			
	a	b	c	$\alpha$	$\beta$	$\Gamma$	Hf	Si	O	Average
0	10.305	10.396	10.589	90.01	99.74	89.97	7.00	...	3.50	4.67
3	10.288	10.351	10.599	90.11	99.48	90.40	6.97	5.00	3.38	4.56
10	10.234	10.221	10.652	90.13	98.99	90.41	7.13	5.00	3.36	4.55
20	10.159	10.036	10.632	90.33	97.94	88.72	7.08	5.33	3.22	4.40
30	9.906	9.803	10.620	87.34	96.17	90.85	6.43	5.18	3.00	4.00
40	9.695	9.438	10.513	91.49	94.12	89.93	6.94	5.38	3.06	4.09

TABLE II. Calculated energy variation for each of the reactions shown: far/close indicates distance from the Si atom. In parentheses are the corresponding values for HfO<sub>2</sub> calculated for the most relevant cases.

#	Reaction	$\Delta E$ (eV)
1a	H(far) $\rightarrow$ H(close)	-0.2
1b	H <sub>2</sub> (far) $\rightarrow$ 2H(close)	-0.4
2a	HfSiO $\rightarrow$ HfSiO(V3) + (1/2)O <sub>2</sub> (gas)	+6.5(+6.8)
2b	HfSiO $\rightarrow$ HfSiO(V4) + (1/2)O <sub>2</sub> (gas)	+6.3(+6.7)
2c	V4(far) $\rightarrow$ V4(close)	-0.2
3a	V3+H(far) $\rightarrow$ V3+H(close)	-1.6(-2.0)
3b	V3+H(close)+H(far) $\rightarrow$ V3+2H(close)	-2.1(-0.8)
3c	V3+H <sub>2</sub> (far) $\rightarrow$ V3+2H(close)	-2.8(-2.6)
3d	V4+H(far) $\rightarrow$ V4+H(close)	-2.3(-2.3)
3e	V4+H(close)+H(far) $\rightarrow$ V4+2H(close)	-2.1(-0.8)
3f	V4+H <sub>2</sub> (far) $\rightarrow$ V4+2H(close)	-3.0(-1.3)
4a	2H(close)+H(far) $\rightarrow$ H(close)+H <sub>2</sub> (close)	-0.7
4b	H(close)+H <sub>2</sub> (far) $\rightarrow$ H(close)+H <sub>2</sub> (close)	+0.2
4c	2H(close)+H <sub>2</sub> (far) $\rightarrow$ 2H(close)+H <sub>2</sub> (close)	+0.0
5a	V4+2H(close)+H(far) $\rightarrow$ V4+3H(close)	-0.9
5b	V4+3H(close)+H(far) $\rightarrow$ V4+2H(close)+H <sub>2</sub> (close)	-0.5
5c	V4+2H(close)+H <sub>2</sub> (close)+H(far) $\rightarrow$ V4+H(close)+2H <sub>2</sub> (close)	-0.9
5d	V4+2H(close)+H <sub>2</sub> (close) $\rightarrow$ V4+2H(close)+H <sub>2</sub> (far)	+0.0

and O5 to three. The remaining three Si–O bonds shorten to 1.73–1.91 Å. The DOS of this configuration [Fig. 4(c)] shows a new gap state  $\sim$ 2.0 eV above the valence band maximum (VBM)<sup>42</sup> associated with the dangling bond in the threefold coordinated Si. The Fermi level (Ef) is at this gap state.

An interstitial H<sub>2</sub> molecule dissociates when placed near the Si atom [Fig. 4(b)]. Besides the H atom that bonds to O6 (O6–H=1.01 Å), the second H atom saturates the Si dangling bond (Si–H=1.44 Å), removing the corresponding gap state [Fig. 4(c)]. The energy gain by moving hydrogen initially far from the Si site to the above-described close-to-Si configurations is 0.2 eV for H and 0.4 eV for H<sub>2</sub> (reactions 1a and 1b in Table II). In HfO<sub>2</sub>, an interstitial H atom adds a state close to the CBM, keeping the gap clean and moving the Fermi level to 1.7 eV [Fig. 4(d)]. This indicates that interstitial H acts as a shallow donor in HfO<sub>2</sub>, in agreement with previous calculations.<sup>15</sup> Further, differently from HfSiO, where H<sub>2</sub> dissociates near the Si site, H<sub>2</sub> dissociation in HfO<sub>2</sub> is endothermic by 0.8 eV.

### C. O vacancies

In order to study O vacancy sites close to the Si atom, we removed O atoms from threefold (V3) and fourfold (V4) coordinated oxygen sites (O6 and O4, respectively). As mentioned earlier, O6 was fourfold coordinated in HfO<sub>2</sub>, but lacks a bond to Si in HfSiO. Thus, V3 is to some extent a transition O vacancy: it is not so close to Si to behave as V4, nor far enough to behave like an O vacancy in HfO<sub>2</sub>. Regarding the structural impact of the vacancy, V3 keeps the fivefold coordination of Si, whereas V4 decreases it to three because the Si–O5 bond is also broken during atomic relaxation.

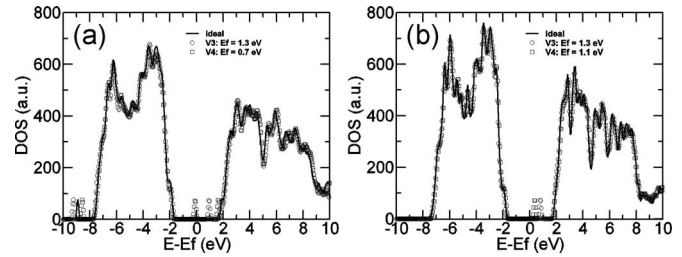


FIG. 5. Density of states of (a) HfSiO and (b) HfO<sub>2</sub> with threefold (V3) and fourfold (V4) coordinated oxygen vacancies.

The DOS for V4 in HfSiO [Fig. 5(a)] shows two gap states: one near midgap and other close to the CBM. Calculations by Xiong *et al.*<sup>39</sup> also derived these two defect states associated with an O vacancy in crystalline HfSiO<sub>4</sub>. The state lying near midgap is localized on Si *sp*<sup>3</sup> orbital, whereas the state lying close to CBM is localized on Hf *d* orbital. This agreement between the DOS for V4 and the O vacancy in HfSiO<sub>4</sub> (Ref. 39) reflects the common origin of these vacancies, involving Hf–O and Si–O bond breakage. V3 formation, on the other hand, does not break any Si–O bond, which leads to a single V3-induced gap state [Fig. 5(a)], resembling the vacancy-induced state for HfO<sub>2</sub> [Fig. 5(b)].

Calculating O vacancy formation energies (reactions 2a and 2b in Table II) is significantly method-dependent due to inaccurate calculation of the O<sub>2</sub> molecule total energy.<sup>43,44</sup> For instance, although the calculated dissociation energy of the O<sub>2</sub> molecule using the SIESTA code is 6.4 eV, its experimental value is only 5.1 eV.<sup>45</sup> In order to address this issue, calculations using an all-solid-state (allSS) method and adding spin polarization (wSP) were performed in addition to the standard calculations (shown in Table II) without spin polarization (woSP). Within the accuracy of the calculations, spin polarization does not influence reaction energies except through the O<sub>2</sub> term. Moreover, the allSS method, which is discussed in detail elsewhere,<sup>46</sup> avoids the troublesome calculation for O<sub>2</sub> by obtaining the O<sub>2</sub> total energy through the equation

$$E_T(\text{O}_2) = E_T(\text{HfO}_2) - E_T(\text{Hf}) - E_F(\text{HfO}_2), \quad (1)$$

where  $E_T(\text{HfO}_2)$  and  $E_T(\text{Hf})$  are calculated total energies for HfO<sub>2</sub> and Hf, respectively, and  $E_F(\text{HfO}_2)$  is the experimental HfO<sub>2</sub> formation energy [11.6 eV/formula at 300 K (Ref. 47)]. Using these methods (woSP/wSP/allSS) for calculating vacancy formation energies in HfO<sub>2</sub>, one obtains 6.8/6.4/6.9 eV for V3 and 6.7/6.2/6.8 eV for V4. These energies compare quite well with the 6.4 eV reported in other studies.<sup>33,48</sup> For HfSiO one obtains formation energies of 6.5/5.9/6.6 eV for V3 and 6.3/6.0/6.3 eV for V4. That is, V3 and V4 in HfSiO are almost equally stable despite the differences in bonding configuration. Moreover, the vacancies in HfSiO are 0.2–0.5 eV more favorable than in HfO<sub>2</sub>, indicating that O vacancies tend to migrate toward close-to-Si sites, which is also pointed out by the 0.2 eV exothermic displacement of V4 from far from Si to its close-to-Si position (reaction 2c in Table II).

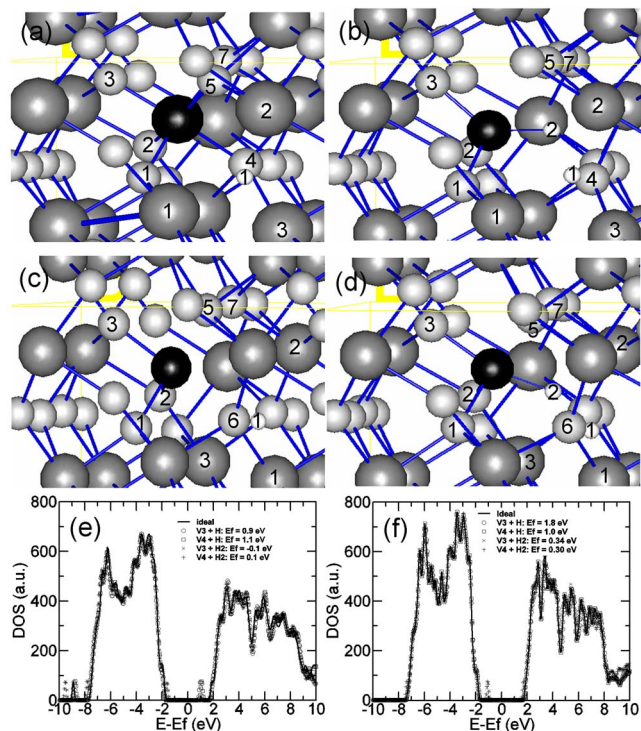


FIG. 6. (Color online) Model structures of HfSiO with (a) H-passivated threefold coordinated O vacancy (V3) and (b) H<sub>2</sub>-passivated V3; model structures of HfSiO with (c) H-passivated fourfold coordinated vacancy (V4) and (d) H<sub>2</sub>-passivated V4; (e) Density of states of HfSiO for the cases from (a)–(d); (f) Density of states of HfO<sub>2</sub> with corresponding O vacancies and H/H<sub>2</sub> passivation.

### D. H and H<sub>2</sub> at O vacancies

An H atom and a H<sub>2</sub> molecule were placed at V4 to understand their interaction with this HfSiO defect. After ionic relaxation, the H atom is close to the vacancy center [Fig. 6(c)], forming a multicenter bond<sup>49</sup> with the neighbor Hf atoms (Hf1–H=2.12 Å, Hf2–H=2.21 Å, Hf3–H=2.23 Å). The Si atom remains threefold coordinated, bonded only to its threefold coordinated O nearest neighbors. The Si–H distance is 2.65 Å. A H<sub>2</sub> molecule dissociates when placed at V4 [Fig. 6(d)]. Besides the H atom [H1 in Fig. 6(d)] close to the vacancy center (Hf1–H=2.12 Å, Hf2–H=2.19 Å, Hf3–H=2.18 Å), the second H saturates the Si dangling bond (Si–H<sub>2</sub>=1.48 Å), bringing the Si coordination to four.

The next defect considered is V3 close to the Si atom. This vacancy site was also occupied with a H atom and a H<sub>2</sub> molecule. After ionic relaxation, the H atom is close to the vacancy center [Fig. 6(a)], forming a multicenter bond<sup>49</sup> with the neighbor Hf atoms (Hf1–H=2.04 Å, Hf2–H=2.07 Å, Hf3–H=2.15 Å). The Si atom is sixfold coordinated due to formation of a bond with O7 during relaxation, though this bond (2.01 Å) is longer than the other five (1.83–1.96 Å). The Si–H distance is 2.92 Å. A H<sub>2</sub> molecule dissociates when placed at V3 [Fig. 6(b)]. Besides the H atom close to the vacancy center (Hf1–H=2.10 Å, Hf2–H=2.13 Å, Hf3–H=2.28 Å), the second H binds to Si (Si–H<sub>2</sub>=1.44 Å). In this case, the proximity of the H atom breaks the Si–O<sub>4</sub>, Si–O<sub>5</sub>, and Si–O<sub>7</sub> bonds, bringing the Si coordination number to four, the same Si coordination observed for V4+H<sub>2</sub>.

Figure 6(e) shows the DOS for HfSiO with H and H<sub>2</sub> at V3 or V4. For both vacancy types two H atoms are necessary to remove the vacancy-induced gap states, though these clear-gap configurations generate edge states at VBM. In HfO<sub>2</sub>, on the other hand, one H atom is enough to clear the gap [Fig. 6(f)]. A H<sub>2</sub> molecule dissociates when placed at V3 or V4 in HfO<sub>2</sub>, creating new gap states near VBM due to the extra H atom. Moreover, comparing V+H complexes in HfO<sub>2</sub> and V+2H complexes in HfSiO, which lead to clear gaps, one notes that V+H in HfO<sub>2</sub> tend to be positively charged [Ef near CBM, Fig. 6(f)], whereas V+2H in HfSiO tend to be neutral [Ef near midgap, Fig. 6(e)].

In HfSiO, the energy gain to bring one H atom from an interstitial site distant from V3/V4 to its relaxed location near the vacancy center is 1.6/2.3 eV (reactions 3a/3d in Table II). A second H is also attracted to V3/V4, with an energy gain of 2.1/2.1 eV (reactions 3b/3e in Table II). Notice that the energy gain to bring a second H to V3/V4 in HfO<sub>2</sub> is considerably lower (0.8/0.8 eV) than in HfSiO. The energy gain for an H<sub>2</sub> molecule to occupy V3/V4 starting from an HfSiO interstitial site is 2.8/3.0 eV (reactions 3c/3f in Table II).

### E. Maximum H uptake near Si

The presence of more than two H atoms near the Si atom in the absence of O vacancies is not favorable. Once two H atoms reside at the Si site, an extra H atom leads to formation of H<sub>2</sub> (reaction 4a in Table II, the energy gain reflects H<sub>2</sub> formation), which is repelled from the Si site (reaction 4b in Table II). Moreover, a H<sub>2</sub> molecule moves freely through the Si site when it is already occupied by two H atoms (reaction 4c in Table II). Considering the presence of more than two H atoms at V4 sites in HfSiO, (reaction 5a in Table II) indicates that a third H atom can be packed in that region, with one H occupying the V4 site, one H bonded to Si, and the third H bonded to O<sub>2</sub>. More than three H atoms at V4 lead to H<sub>2</sub> formation, with corresponding energy gains (reactions 5b and 5c in Table II). Interstitial H<sub>2</sub> moves freely through V4 + 2H (reaction 5d in Table II).

## V. DISCUSSION

The tendency of O vacancy migration toward Si atoms, as indicated by the lower vacancy formation energy in HfSiO than in HfO<sub>2</sub> (reactions 2a–2c in Table II), implies that oxygen deficiency in HfSiO tend to manifest as suboxidized Si atoms, which leads to Si 2*p* peaks shifted toward lower binding energies, as observed in Fig. 2. This tendency was also experimentally<sup>50,51</sup> and theoretically<sup>48</sup> established for the extreme case of phase-separated SiO<sub>2</sub> and HfO<sub>2</sub>, where O vacancies tend to move toward the SiO<sub>2</sub> side of a HfO<sub>2</sub>/SiO<sub>2</sub> interface.

Considering H trapping, the calculated exothermic H capture at O vacancies (reactions 3a–3f in Table II) clearly supports the experimentally observed correlation between <sup>2</sup>H incorporation (Fig. 1) and O deficiency (Fig. 2). Nevertheless, in order to better understand the link between theory and experiment, it is worth referencing the reaction energies from Table II to a free H<sub>2</sub> molecule. The energy necessary to

move a free H<sub>2</sub> molecule into an interstitial site in HfO<sub>2</sub> is 1.6 eV,<sup>16</sup> where H<sub>2</sub> dissociation costs additional 0.8 eV. Hence, the formation energy of one H interstitial in HfO<sub>2</sub> is 1.2 eV. Noting that the word “far” in Table II refers to HfO<sub>2</sub>-like regions, adding 1.6/1.2 eV for each H<sub>2</sub>(far)/H(far) reactant results in H trapping energies referenced to free H<sub>2</sub>. With this reference, a second H atom at a vacancy in HfO<sub>2</sub> ( $\Delta E = -0.8$  eV, reactions 3b and 3e in Table II) as well as a third H atom at a vacancy in HfSiO ( $\Delta E = -0.9$  eV, reaction 5a in Table II) become endothermic when adding the 1.2 eV to account for H(far) formation. Hence, the maximum number of energetically favored trapped H atoms at an O vacancy becomes one in HfO<sub>2</sub> and two in HfSiO.

These energetically favored configurations (V+H in HfO<sub>2</sub> and V+2H in HfSiO) are also the configurations leading to clear band gaps [Figs. 6(e) and 6(f)]. That is, these favored H-containing configurations are electrically inactive. Indeed, considering that typical H areal densities in Hf-based films ( $\sim 10^{15}$  cm<sup>-2</sup>) (Refs. 17–19) are much higher than the areal densities of electrically active defects in such structures ( $10^{11}$ – $10^{13}$  cm<sup>-2</sup>),<sup>1–3</sup> one infers that H sites, *in general*, tend to be electrically inactive. However, as observed for SiO<sub>2</sub>,<sup>7,8,11</sup> radioactive, thermal, and electrical stress might detrapp the H atoms, activating the defects and generating instabilities in the MOSFET.

## VI. CONCLUSIONS

In summary, using annealing sequences, nuclear reaction analysis, x-ray photoelectron spectroscopy, and first-principles density-functional calculations, H trapping in O-deficient hafnium silicates was investigated. The experiments showed that O-deficient HfSiO films tend to incorporate H atoms. Supplying O to the films reduces H incorporation presumably due to removal of the O-deficient sites that trap H. The calculations were performed in a HfSiO model with one Si atom replacing one Hf atom in the *m*-HfO<sub>2</sub> structure. They showed that close-to-Si O vacancies are energetically favored in comparison with O vacancies in HfO<sub>2</sub>-like regions, indicating that close-to-Si vacancies are more likely to occur. Exothermic trapping of one and two H atoms at these close-to-Si vacancy sites was calculated, providing a theoretical basis for the experimentally observed relationship between H incorporation and O deficiency. Finally, it was verified that two H atoms at the vacancy remove the vacancy-induced gap states. The first H atom forms a multicenter bond with neighbor Hf atoms, whereas the second H binds to the Si atom.

## ACKNOWLEDGMENT

The authors thank Andrey Knizhnik for helpful discussions and suggestions.

<sup>1</sup>J. Robertson, Rep. Prog. Phys. **69**, 327 (2006).

<sup>2</sup>*High-κ Gate Dielectrics*, edited by M. Houssa (Institute of Physics, Bristol, 2004).

<sup>3</sup>G. D. Wilk, R. M. Wallace, and J. M. Anthony, J. Appl. Phys. **89**, 5243 (2001).

<sup>4</sup>G. D. Wilk and R. M. Wallace, Appl. Phys. Lett. **74**, 2854 (1999).

<sup>5</sup>G. D. Wilk, R. M. Wallace, and J. M. Anthony, J. Appl. Phys. **87**, 484 (2000).

<sup>6</sup>K. L. Brower, Phys. Rev. B **38**, 9657 (1988).

<sup>7</sup>D. K. Schroder and J. A. Babcock, J. Appl. Phys. **94**, 1 (2003).

<sup>8</sup>D. M. Fleetwood, Microelectron. Reliab. **42**, 523 (2002).

<sup>9</sup>J. Dimaria and E. Cartier, J. Appl. Phys. **78**, 3883 (1995).

<sup>10</sup>P. E. Blochl and J. H. Stathis, Phys. Rev. Lett. **83**, 372 (1999).

<sup>11</sup>J. W. Lyding, K. Hess, and I. C. Kizilyalli, Appl. Phys. Lett. **68**, 2526 (1996).

<sup>12</sup>A. Y. Kang, P. M. Lenahan, J. F. Conley, and R. Solanki, Appl. Phys. Lett. **81**, 1128 (2002).

<sup>13</sup>A. Stesmans and V. V. Afanas'ev, Appl. Phys. Lett. **82**, 4074 (2003).

<sup>14</sup>M. Houssa, V. V. Afanas'ev, A. Stesmans, and M. M. Heyns, Appl. Phys. Lett. **77**, 1885 (2000).

<sup>15</sup>P. W. Peacock and J. Robertson, Appl. Phys. Lett. **83**, 2025 (2003).

<sup>16</sup>J. Kang, E. C. Lee, K. J. Chang, and Y. G. Jin, Appl. Phys. Lett. **84**, 3894 (2004).

<sup>17</sup>R. P. Pezzi *et al.*, Appl. Phys. Lett. **85**, 3540 (2004).

<sup>18</sup>C. Driemeier, L. Miotti, I. J. R. Baumvol, C. Radtke, E. P. Gusev, M. J. Kim, and R. M. Wallace, Appl. Phys. Lett. **88**, 041918 (2006).

<sup>19</sup>C. Driemeier, J. J. Chambers, L. Colombo, and I. J. R. Baumvol, Appl. Phys. Lett. **89**, 051921 (2006).

<sup>20</sup>S. M. Myers, J. Appl. Phys. **61**, 5428 (1987).

<sup>21</sup>J. Krauser, A. Weidinger, and D. Bräuning, in *The Physics and Chemistry of SiO<sub>2</sub> and of the Si/SiO<sub>2</sub> Interface—3*, edited by H. Z. Massoud, E. H. Poindexter, and C. R. Helms (The Electrochemical Society, Pennington, NJ, 1996), E.U.A. Vol. 96-1, pp. 59–71.

<sup>22</sup>M. Wilde, M. Matsumoto, K. Fukutani, Z. Y. Liu, K. Ando, Y. Kawashima, and S. Fujieda, J. Appl. Phys. **92**, 4320 (2002).

<sup>23</sup>I. J. R. Baumvol, E. P. Gusev, F. C. Stedile, F. L. Freire, Jr., M. L. Green, and D. Brasen, Appl. Phys. Lett. **72**, 450 (1998).

<sup>24</sup>A. Van Wieringen and N. Warmoltz, Physica **22**, 849 (1956).

<sup>25</sup>W. Möller and F. Besenbacher, Nucl. Instrum. Methods **168**, 111 (1980).

<sup>26</sup>C. Driemeier, R. M. Wallace, and I. J. R. Baumvol, J. Appl. Phys. **102**, 024112 (2007).

<sup>27</sup>Relative binding energies of Hf 4*f* and Si 2*p* peaks were referenced to binding energies of the corresponding O 1*s* peaks. This approach assures that binding energy shifts are of chemical nature and are not due to x-ray-induced charges.

<sup>28</sup>J. P. Perdew and Y. Wang, Phys. Rev. B **45**, 13244 (1992).

<sup>29</sup>P. Hohenberg and W. Kohn, Phys. Rev. **136**, B864 (1964); W. Kohn and L. J. Sham, *ibid.* **140**, A1133 (1965).

<sup>30</sup>J. M. Soler, E. Artacho, J. D. Gale, A. Garcia, J. Junquera, P. Ordejon, and D. Sanchez-Portal, J. Phys.: Condens. Matter **14**, 2745 (2002).

<sup>31</sup>W. C. Topp and J. J. Hopfield, Phys. Rev. B **7**, 1295 (1973).

<sup>32</sup>N. Troullier and J. L. Martins, Phys. Rev. B **43**, 1993 (1991).

<sup>33</sup>A. S. Foster, F. Lopez Gejo, A. L. Shluger, and R. M. Nieminen, Phys. Rev. B **65**, 174117 (2002).

<sup>34</sup>R. Ruh and P. W. R. Corfield, J. Am. Ceram. Soc. **53**, 126 (1970).

<sup>35</sup>The cutoff length for bond counting is 1.1 times the sum of the two covalent radii.

<sup>36</sup>C. R. Helms and E. H. Poindexter, Rep. Prog. Phys. **57**, 791 (1994).

<sup>37</sup>S. Mukhopadhyay, P. V. Sushko, A. M. Stoneham, and A. L. Shluger, Phys. Rev. B **70**, 195203 (2004).

<sup>38</sup>P. Broqvist and A. Pasquarello, Appl. Phys. Lett. **90**, 082907 (2007).

<sup>39</sup>K. Xiong, Y. Du, K. Tse, and J. Robertson, J. Appl. Phys. **101**, 024101 (2007).

<sup>40</sup>G. Lucovsky, J. Vac. Sci. Technol. A **19**, 1553 (2001).

<sup>41</sup>S. Sayan, E. Garfunkel, and S. Suzer, J. Appl. Phys. **80**, 2135 (2002).

<sup>42</sup>Due to the band gap underestimation in DFT, the exact location of the defect states in the gap cannot be determined within this approach. Therefore the energies of the gap states only indicate trends.

<sup>43</sup>A. Eichler, F. Mittendorfer, and J. Hafner, Phys. Rev. B **62**, 4744 (2000).

<sup>44</sup>I. G. Batyrev, A. Alavi, and M. W. Finnis, Phys. Rev. B **62**, 4698 (2000).

<sup>45</sup>P. Brix and G. Herzberg, Can. J. Phys. **32**, 110 (1954).

<sup>46</sup>A. V. Gavrikov, A. A. Knizhnik, A. A. Bagatur'yants, B. V. Potapkin, L. R. C. Fonseca, M. W. Stoker, and J. Schaeffer, J. Appl. Phys. **101**, 014310 (2007).

<sup>47</sup>*Thermodynamic Properties of Individual Substances, Reference Book*, edited by V. P. Glushko (Nauka, Moscow, 1978).

<sup>48</sup>W. L. Scopel, A. J. R. da Silva, W. Orellana, and A. Fazzio, Appl. Phys. Lett. **84**, 1492 (2004).

<sup>49</sup>A. Janotti and C. G. Van de Walle, Nat. Mater. **6**, 44 (2007).

<sup>50</sup>M. Copel and M. C. Reute, Appl. Phys. Lett. **83**, 3398 (2003).

<sup>51</sup>G. Bersuker *et al.*, J. Appl. Phys. **100**, 094108 (2006).